Magazine of Civil Engineering

ISSN 2712-8172

journal homepage: http://engstroy.spbstu.ru/

Research article

UDC 624.21/.8

DOI: 10.34910/MCE.135.3

Aeroelastic vibrations of arch bridge suspensions

Yu.A. Gosteev ✉ **, *I.S. Konovalov, A.D. Obuhovskiy, S.D. Salenko***

Novosibirsk State Technical University (NSTU), Novosibirsk, Russian Federation

✉ *gosteev@corp.nstu.ru*

Keywords: aeroelastic vibrations, vortex-induced vibrations, galloping, aerodynamics of bridges, section model, cantilever model, wind loads

Abstract. The article identifies the causes of aeroelastic vibrations of suspensions on the arch bridge with the main span of more than 200 m. The study aims to determine the range of dangerous wind speeds and maximum amplitudes of these vibrations. This research is necessary due to intense vibrations of suspensions on the operated structure at wind speeds of 10÷15 m/s. The authors have studied models of bridge span structure and suspensions. Experimental tests as well as flow calculations using application packages have been carried out in the wind tunnel at NSTU. The study has provided verification of the vibration calculation method in the recently approved Russian regulations and comparison of the calculation with the current European method. It has been found that the cause of vibrations of the bridge suspensions is vortex-induced vibrations (VIV), while the central span of the bridge is not subject to aeroelastic vibrations. The experimental results coincide with the calculations and observations of the behavior of the suspensions of the bridge under moderate crosswind. The obtained results will be used in the future to develop methods of suspension vibration damping.

Acknowledgements: The authors would like to thank D.A. Krasnorutskiy for his cooperation in carrying out modal calculations on span structure and its elements.

Citation: Gosteev, Yu.A., Konovalov, I.S., Obuhovskiy, A.D., Salenko, S.D. Aeroelastic vibrations of arch bridge suspensions. Magazine of Civil Engineering. 2025. 18(3). Article no. 13503. DOI: 10.34910/MCE.135.3

1. Introduction

The investigation of bridges as complete systems and their individual structural components – particularly suspensions – became essential with the advent of long-span bridge construction. Due to the length of the span structures, it is not possible to make them sufficiently rigid, therefore, such structures as cable-stayed and arched are used. One of the promising directions of building is using polymer materials for the base of bridges, which have some advantages over reinforced concrete structures [1]. In addition, there is also a risk of occurring aeroelastic vibrations during bridge constructing while launching spans [2]. Poorly streamlined bodies such as elastic long-rod suspensions can occur in bridge structures. The cross-sections of these elements can be cylindrical, rectangular, square, etc. The dynamic interaction of such cross-sections with the air flow has been studied by many authors both in Russia [3, 4] and abroad [5–14]. [15] described a similar case of aeroelastic vibrations for cylindrical suspensions of an arch bridge and ways to reduce vibrations. The relevance of research in this area is supported by using modern computational fluid dynamics (CFD) tools with artificial neural networks [16] for designing bridge and high-rise building.

In addition to studies of the interaction of poorly streamlined bodies with the air flow, there are also studies, which aim to find effective ways to dampen vibrations or, at least, reduce their intensity. For example, [17, 18] presented the passive ways to reduce vortex-induced vibrations (VIV) on a circular cylinder by means of a perforated surface. For a square prism, the paper [19] investigated a method to reduce wind load by rounding edges. [20] described corner fins installment that is another way (both passive and active) to reduce VIV. The paper [21] proposed an interesting way of active wind load control, which can be used for high-rise buildings. The present work deals with the problem of occurring suspension vibrations in bridges caused by the interaction of the suspensions with the wind flow.

Based on the external geometric shapes of the span structures section (Fig. 1) it can be suggested that the structure may be subject to aeroelastic vibrations such as VIV and stall flutter. The cross-section shape of the suspensions (Fig. 2) allows to suggest that they may be subject to aeroelastic vibrations such as VIV and galloping.

Possible causes of suspension vibrations are aerostatic vibrations of:

1) the suspensions in the wind flow;
2) the span structures in the wind flow;
3) the span structures due to road traffic.

The purposes of this research are:

- to study the mechanism of occurrence and development of aeroelastic vibrations of bridge elements;
- to determine the range of wind velocities, at which dangerous aeroelastic vibrations of elements may occur;
- to estimate maximum vibration amplitudes to find ways to reduce aeroelastic vibrations.

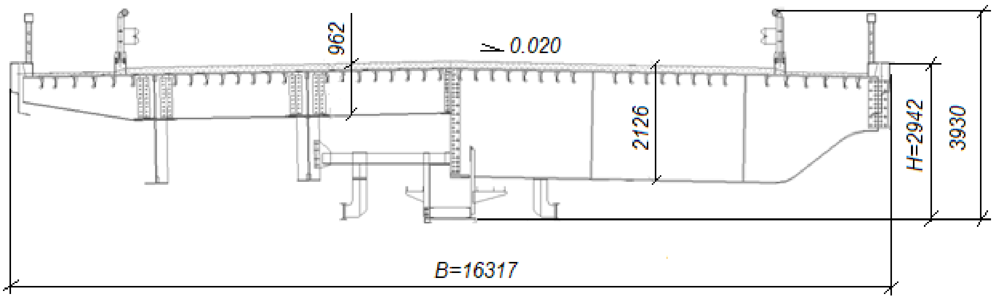

Figure 1. Cross-section of the span structures around the studied suspensions.

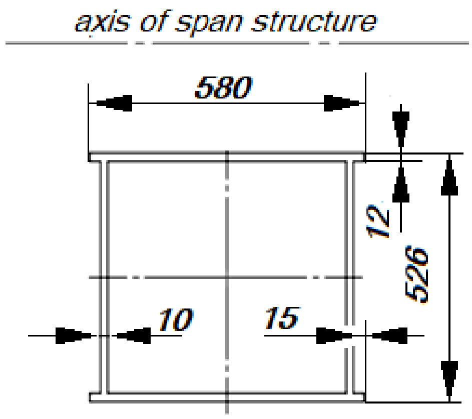

Figure 2. Cross-section of suspensions.

2. Methods

2.1. Preliminary Calculations

For preliminary assessment of the vibration characteristics, the frequencies and shapes of natural vibrations of the bridge were calculated, the shapes of suspension vibrations were identified for further analysis of aeroelastic vibrations.

As a result of calculations, two tones were identified, which were confirmed by full-scale measurements. The 30th tone of natural vibrations corresponds to the frequency of suspension vibrations along the span structure bridge; the frequency equals $f_y =$ 2.88 Hz. The frequency and shape of vibrations have been confirmed by full-scale measurements at a wind speed of 10–12 m/s and with the direction close to perpendicular to the span structures. The calculations have also showed vibrations of suspensions across the span structures. They correspond to the 60th tone and the frequency $f_x =$ 3.82 Hz.

Numerical calculations of the cross-flow of a fixed suspension model with the wind direction across the span structure ($\alpha = 0°$) showed the presence of a track of vortices descending from the surface of the model (Fig. 3). Spectral analysis of fluctuations of the lifting force acting on the model revealed the main frequency, corresponding to the frequency of the vortices shedding with the Strouhal number $Sh_a = 0.13$. At the natural vibration frequency of the suspension $f_y = 2.88$ Hz, the critical wind speed on the middle of the suspension is $V_{cr,y} = f_y H / Sh_a = 12.8$ m/s.

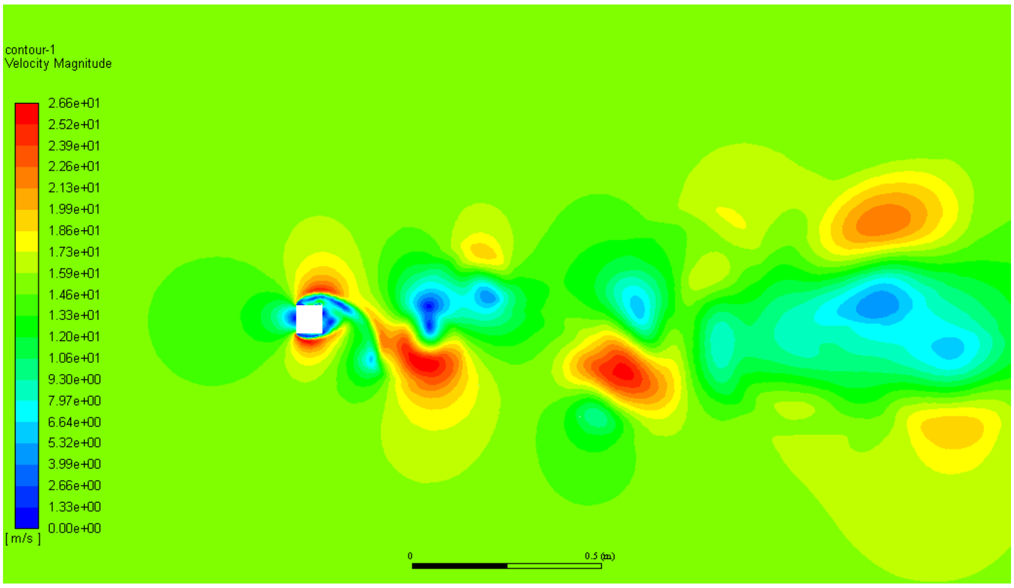

Figure 3. Velocity isolines at *t* = 1 s.

A preliminary assessment of the maximum vibration amplitudes was carried out according to the GOST[1] and Eurocode[2].

Initially, height and width of the cross-section suspension are $H =$ 0.580 m and $B =$ 0.526 m, linear mass is $m =$ 188 kg/m, logarithmic decrement of damping is $\delta =$ 0.02, Strouhal number is $Sh = Sh_a = 0.13$, air density is $\rho =$ 1.225 kg/m³.

According to the methodology described in GOST[3], equation used to estimate the maximum relative amplitude is:

$$\bar{A}_{\max} = 0.7 \frac{B}{H} \frac{1}{\mathrm{Sc}} \frac{1}{\mathrm{Sh}^2} Kc_{\mathrm{a,max}},$$

where $\mathrm{Sc} = 2m_e\delta / (\rho H^2)$ is the Scruton number, m_e is the equivalent linear mass of the span structure or its element (if a uniform mass distribution is $m_e = m$), δ is the logarithmic decrement of damping of the

[1]. Federal Agency on Technical Regulating and Metrology (Rosstandart). Automobile roads of the general use. Bridge constructions. The rules of the aeroelastic stability. Calculation and verification. GOST R 59625–2022. 2022. 42 p.

[2] European Committee for Standardization (CEN). Eurocode 1: Actions on structures – Part 1–4: General actions – Wind actions. EN 1991-1-4:2005. 2005. 146 p.

[3] Federal Agency on Technical Regulating and Metrology (Rosstandart). Automobile roads of the general use. Bridge constructions. The rules of the aeroelastic stability. Calculation and verification. GOST R 59625–2022. 2022. 42 p.

span structure or its element, $\mathrm{Sh} = fH / V$ is the Strouhal number, depending on the cross-section shape and relative width B / H of the span structure section or its element; K is the modal shape factor, K = 0.1 ([21], Appendix B, Table B.1); $c_{a,max}$ is the maximum value of the exciting aerodynamic coefficient, without experimental data it is allowed to take $c_{a,max} = 0.1$.

As a result, the following values of maximum amplitudes have been obtained: according to the GOST[4], $\overline{A}_{\max} = 0.021$, $A_{\max} = 0.012$ m, according to the Eurocode[5], $\overline{A}_{\max} = 0.092$, $A_{\max} = 0.053$ m.

2.2. Model Description

To study the dependencies of relative vibrations amplitudes on the reduced velocity (amplitude-velocity characteristics, AVC), two identical suspension models with different methods of fixing in a wind tunnel have been used: spring-fixed suspension model and cantilever-fixed model. The cross-section of both models is made to a scale of 1:7.5, the length of the models is 600 mm, the aspect ratio is λ = 7.8. To maintain two-dimensional flow conditions, end plates with a diameter of 300 mm have been positioned at the ends of the models. [22] described the effect of the end plates in more detail. The model on a spring elastic suspension (Fig. 4) is fixed in the working section of the wind tunnel with end plates and has 8 spring-loaded attachment points. Four springs are located on one side of the model and connected to elastic elements with strain gauges. The installation allows to record the movements of the model in the longitudinal and transverse direction of the flow and torsional movements in the pitch angle. The beam of the model is fixed between the end plates on both sides by clamping elements, which allows to change the orientation of the model in the flow according to the attack angle.

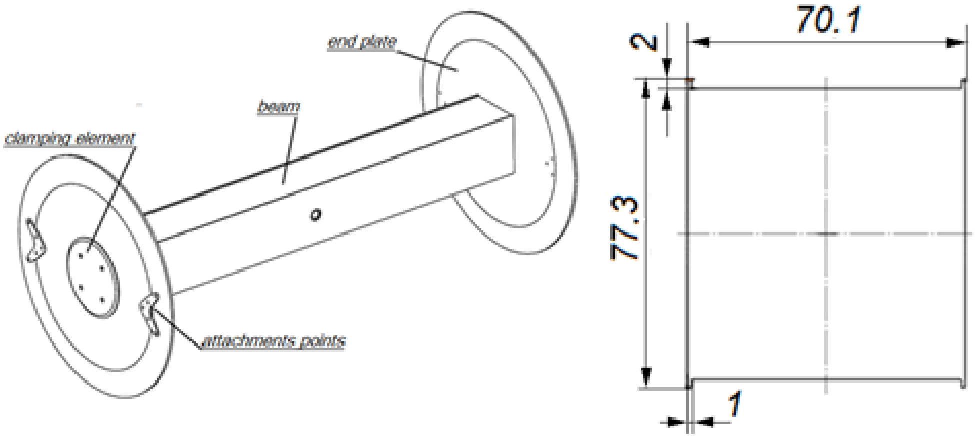

Figure 4. Model general view and cross-section dimensions.

This type of attachment for the model in the wind tunnel test is quite simple and convenient. However, the natural frequency of the elastic suspension is constant, when the attack angle of the model changes, which actually occurs as the wind direction changes. In fact, the full-scale suspension of the bridge has different mechanical rigidity in perpendicular directions and different frequencies of natural vibrations in the first tone, equal to $f_{xn} = 3.82$ Hz and $f_{yn} = 2.88$ Hz, the ratio is $f_{yn} / f_{xn} = 0.75$. It is difficult to ensure the constancy of f_{yn} / f_{xn} on an elastic suspension over the entire range of attack angles. For simulating the frequency ratio, a cantilever-fixed model has been made (Fig. 5). The model is installed on a rigid fixed base outside the wind tunnel with an elastic element. The role of elastic element is performed by a girder milled from aluminum D16T with an I-beam profile, so the natural frequency ratios of the model are $f_{xm} = 18.2$ Hz and $f_{ym} = 13.3$ Hz, $f_{ym} / f_{xm} = 0.73$; and deviations from the natural frequency ratio of the full-scale suspension are 3 %.

[4] Ibid.

[5] European Committee for Standardization (CEN). Eurocode 1: Actions on structures – Part 1–4: General actions – Wind actions. EN 1991-1-4:2005. 2005. 146 p.

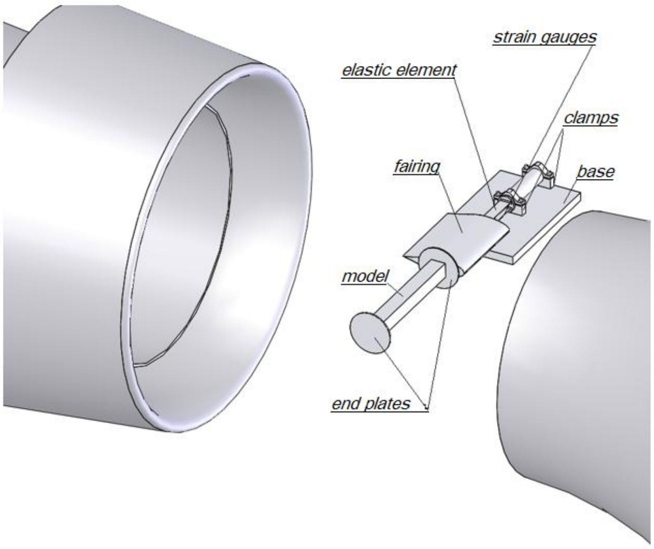

Figure 5. General view of a cantilever-fixed model.

Furthermore, a model of the span structure bridge was made to evaluate AVC, since the suspension vibrations can be caused by vibrations of the span structure in the wind flow. The method of fixing the model in the wind tunnel test and the experimental conditions are the same as for the suspension model of the bridge installed on an elastic suspension.

The Reynolds numbers for models and full-scale structures are in the region of self-similarity of the flow, which is in the range of Reynolds numbers ($10^4 < \mathrm{Re} < 10^7$), so their aerodynamic characteristics have not undergone significant changes.

3. Results and Discussion

3.1. AVC of Span Structure Model on an Elastic Spring Suspension

The investigation began with aerodynamic testing of the span structure model to identify potential causes of bridge suspension vibrations. The obtained AVC are shown on dimensionless graphs. The relative amplitude of the investigated model $\overline{A} = A/H$ is plotted along the vertical axis; where *A* is the amplitude of the model, *H* is the overall height of the model, and the relative velocity equals to $\overline{V} = 1/\mathrm{Sh}$ or $\overline{V} = V/(fH)$ plotted along the horizontal axis. The results of the aerodynamic experiments, presented in Fig. 6, showed the absence of intense vibrations of the span structure model at all tested velocities, corresponding to the natural wind speed at $V_{\max} = 1.5V_{\mathrm{calc}}$ at span level. The amplitudes of vertical vibrations of the span structure at the $V_{\max}$ speed did not exceed 18 mm in terms of a full-scale structure. This suggests that the span structure vibrations cannot be the cause of intense suspension vibrations.

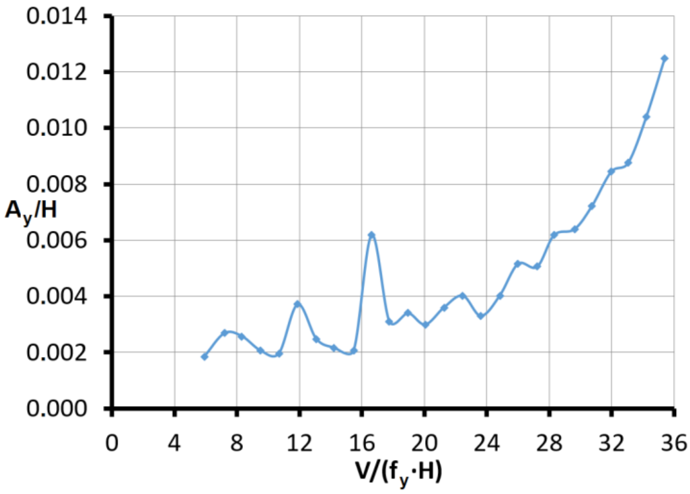

Figure 6. AVC of the span structure model on elastic suspension.

3.2. AVC of Suspension Models of the Bridge on Elastic Suspension

The aerodynamic experiment was conducted in the T-503 open wind tunnel under the following conditions: turbulence intensity $\varepsilon \approx 0.3\%$ in steady flow; flow velocity varied from 5 to 20 m/s; Reynolds numbers equal to 2.5·(10^4÷10^5), in the range of self-similarity; flow velocity stability was ±0.5 %. AVC measurements are recorded for 0°, 45°, 90° angles of attack (Fig. 7); for the vibration amplitudes in the direction across the flow, the logarithmic decrement of damping is $\delta \approx 0.007$. For the convenience of recalculating velocities and amplitudes to full-scale dimensions, the AVC graphs are given in dimensionless form (Fig. 8). The vibrations were unstable, the oscillogram signal was averaged to the standard deviation and multiplied by the coefficient $\sqrt{2}$. [23] described a similar method of processing the received amplitude signals in detail.

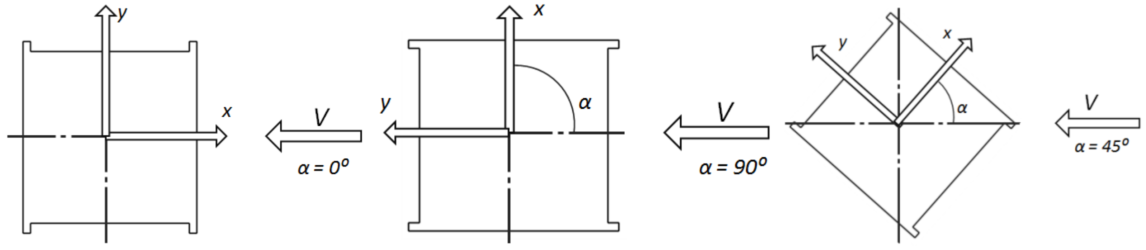

Figure 7. Attack angles of the model.

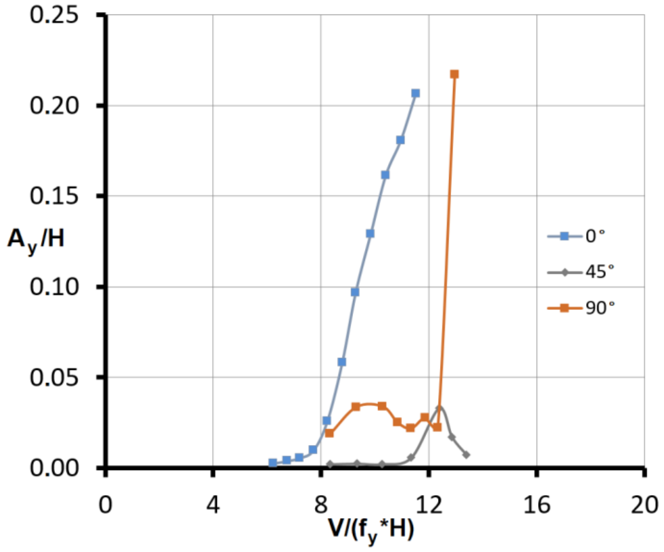

Figure 8. AVC of the sectional suspension model ($\alpha = 0°…90°$).

From the graphs, it can be seen that at a relative velocity $\overline{V} = 8$, corresponding to the Strouhal number $\mathrm{Sh} = 0.125$, and at an angle of attack $\alpha = 0°$, appearing vibrations gradually increase to a relative amplitude $\overline{A} = 0.2$ at a relative velocity $\overline{V} = 11.5$. The experiment could not be conducted at higher speeds due to the risk of damaging the elastic suspension elements. When the model is positioned at α =90°, the relative amplitude does not exceed the value of $\overline{A} = 0.03$ up to the relative velocity $\overline{V} = 12.5$. The amplitude increases with speed. The same Strouhal number values were observed when the model was positioned at $\alpha = 45°$. In this position, an insignificant amplitude maximum was observed.

The aerodynamic experiments on elastic suspension with various damping degrees were carried out at the angle of attack $\alpha = 0°$ (Fig. 9). For this purpose, stepped dampers of various diameters, similar in shape to spherical ones, were fixed to the middle of the lower surface of the model on a vertical spoke. The increase in the weight of the model due to the damper installation was less than 1%. The damping was carried out in a viscous fluid, which made it possible to conduct aerodynamic experiments at higher speeds without damage to the suspension elements of the model.

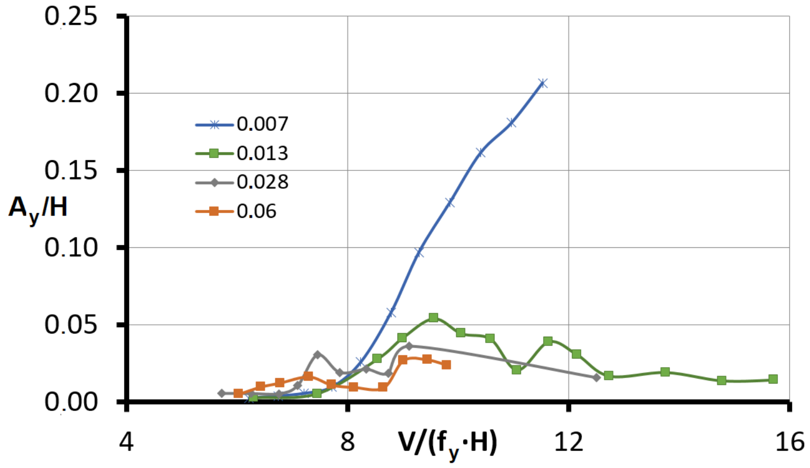

Figure 9. AVC models on an elastic suspension with different vibration decrements of damping ($\delta = 0.007 \ldots 0.06$).

From the graphs, it can be seen that the maximum of the amplitude is observed at a relative velocity $\overline{V} = 10.5$, at the value of the vibration decrement of damping $\delta = 0.013$. The vibration amplitude decreases at higher speeds.

3.3. AVC of the Cantilever-fixed Bridge Suspension Model

The experimental conditions for the cantilever-fixed model are the same as for the elastic suspension model. However, this configuration has the following parameters: the rigidity ratio, the natural vibration frequencies along both axes of the model cross-section, and the strength of the elastic beam in the experimental setup. This allowed us to measure the amplitude of the vibrations in the model over the entire range of operating speeds. Aerodynamic wind tunnel tests were carried out at attack angles $\alpha = (0 \div 90)°$ with a step of (5÷10)°, without additional damping. AVC results for two extreme and one average values of $\alpha = 0°, 45°, 90°$ are shown in Fig. 10. The logarithmic decrements of damping for $\alpha = 0°$ are $\delta_y = 0.006$ and for $\alpha = 90°$ are $\delta_x = 0.0065$.

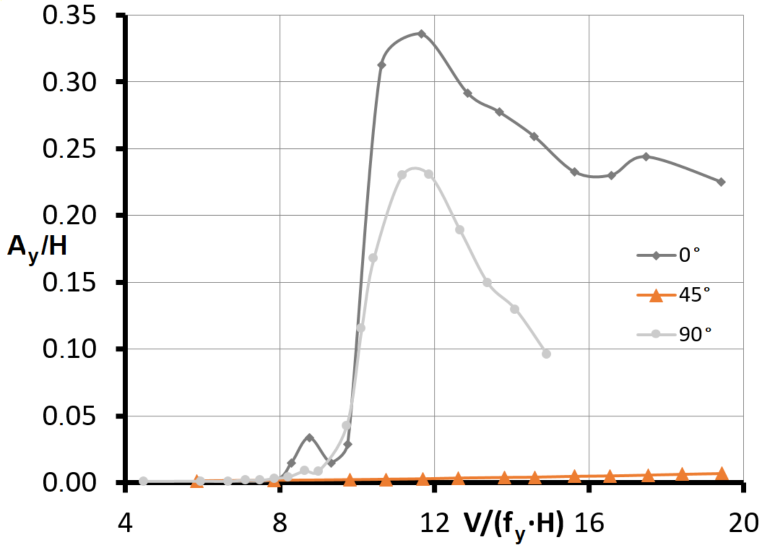

Figure 10. AVC of the cantilever-fixed model perpendicular to the flow ($\alpha = 0° \ldots 90°$).

The maximum relative amplitude for vibrations along the OY axis of the model is $\overline{A} = 0.34$, as the amplitude along the OX axis is $\overline{A} = 0.24$. Unstable vibrations with small amplitudes occur at relative velocity $\overline{V} = 8$ and higher. When the relative velocity $\overline{V} = 9 \div 10$ is reached, the amplitude increases significantly and reaches its maximum values. In the relative velocities $\overline{V} = 8 \div 10$, hysteresis is also observed. [24] noted a similar phenomenon for galloping a rectangular prism with aspect ratio up to $\lambda = 10$. The critical Strouhal number for the model at angles of attack $\alpha = 0°$ and $\alpha = 90°$ was $\mathrm{Sh} = 0.086$. After reaching the maximum rate without additional damping of the model, the amplitude decreases but remains significant, which is probably due to the transition to galloping. At the attack angle $\alpha = 45°$, no noticeable vibrations were detected in any directions.

The measured logarithmic damping decrement of full-scale suspension vibrations of the bridge, when the wind direction is perpendicular to the bridge, equals to $\delta = 0$. However, according to GOST[6], the value $\delta = 0.02$ was taken for calculation. The experiments were conducted with different damping degrees of the model for determining the dependence of the exciting aerodynamic force coefficient on the relative amplitude (Figs. 11 and 12). Further experiments were conducted due to the significant difference among the decrements of the cantilever-fixed model from the value.

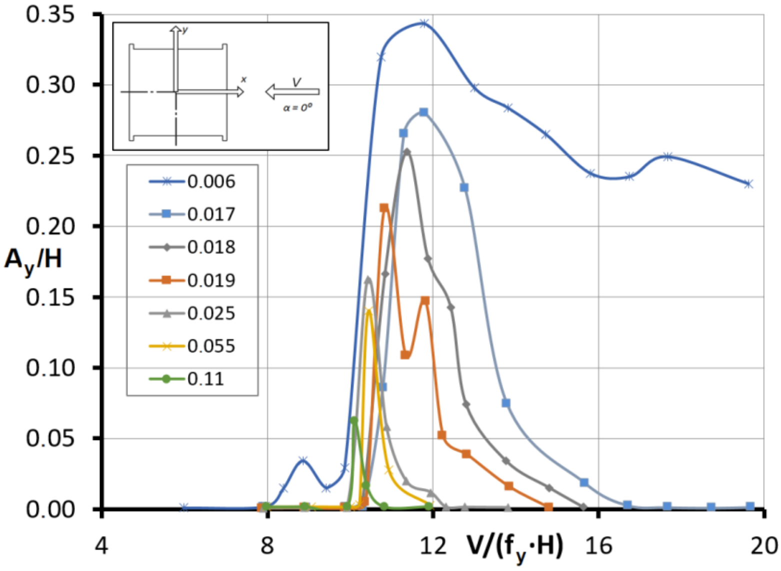

Figure 11. Damping effect on the AVC of the cantilever-fixed model when the wind direction is perpendicular to the span of the bridge ($\delta = 0.006…0.11$).

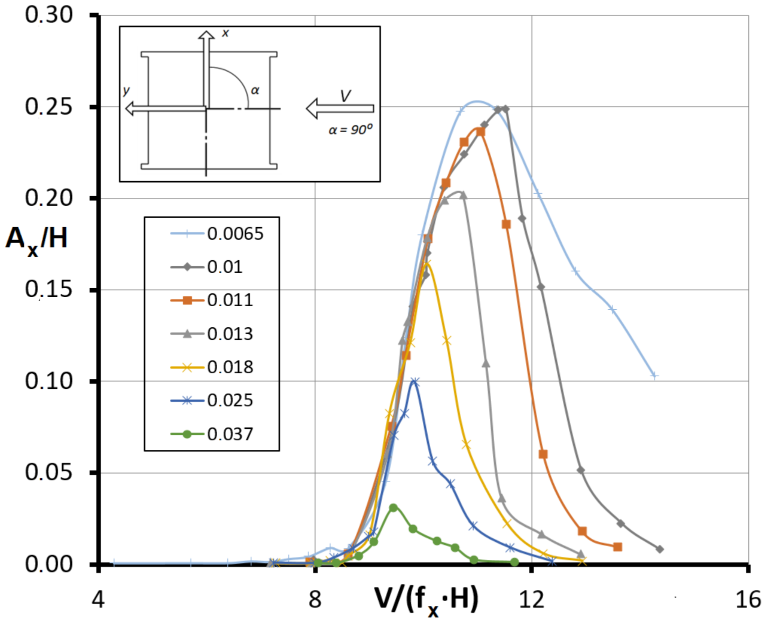

Figure 12. Damping effect on the AVC of the cantilever-fixed model when the wind direction is parallel to the bridge span ($\delta = 0.0065…0.037$).

[6] Federal Agency on Technical Regulating and Metrology (Rosstandart). Automobile roads of the general use. Bridge constructions. The rules of the aeroelastic stability. Calculation and verification. GOST R 59625–2022. 2022. 42 p.

Table 1. Logarithmic decrement of damping models with different damping degrees.

No. of the damper	Without a damper	D3	D4	D5	D5,5	D6	D7
$\delta_x(A_{max})$	0.0065	0.010	0.011	0.013	0.018	0.025	0.037
$\delta_y(A_{max})$	0.006	0.017	0.018	0.019	0.025	0.055	0.11

When $\delta = 0.02$, as taken from GOST[7], and using the method of amplitude measurement for the cantilever-fixed model applied in this study, the relative amplitude is $\overline{A}_{\max} = 0.22$. This value differs from the calculated one, specified in the same GOST, ($\overline{A}_{\max} = 0.21$) by only 4 %.

When measured on a full-scale suspension $\delta = 0.015$ and average amplitude of about 70 mm with a wind speed of ≈12 m/s, the measured relative amplitude is $\overline{A}_{\max} = 0.12$. This is two times lower than the experimental and calculated amplitude. This can be related to the unstable direction (±10° from perpendicular direction to the span structure) and wind speed observed in full-scale conditions.

Based on the cantilever-fixed model experiment results, the dependences of the aerodynamic exciting coefficients c_a on the relative amplitude (Fig. 13) $c_{a,y}\left(\overline{A}_y\right)$ and $c_{a,x}\left(\overline{A}_x\right)$ were determined according to the method described in GOST[8]. The coefficient c_a is used to calculate the maximum relative amplitude of the vibrations.

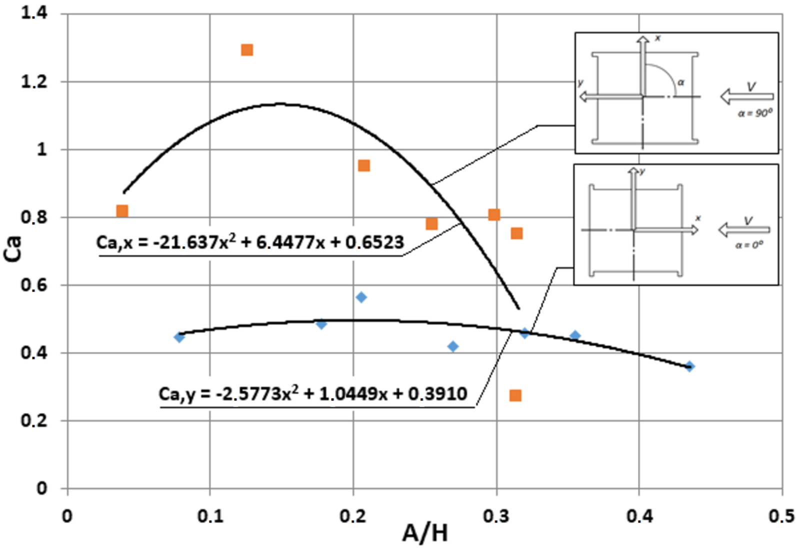

Figure 13. Dependence of the aerodynamic exciting coefficients $c_{a,y}$ and $c_{a,x}$ on the relative amplitude of the vibrations.

4. Conclusions

1. When investigating the causes of aeroelastic vibrations of the bridge, calculations and experiments have revealed that the wind resonance of the suspensions of a bridge is the main cause of these vibrations.
2. The span of the bridge is not subject to dangerous aeroelastic vibrations. At the same time, the range of VIV velocity at the level of suspensions has found to be 12÷18 m/s. It indicates the frequent occurrence of aeroelastic vibrations, which requires finding ways to reduce vibrations on the building in operation.

---

[7] Ibid.

[8] Ibid.

3. New data on the aerodynamic characteristics of an H-shaped section, geometrically similar to a square section, have been obtained. The results show that a slight difference from a well-studied square section leads to significant changes in the aerodynamic exciting coefficient. And the aerodynamic exiting coefficient differs by more than two times for angles of attack of 0° and 90° for the H-shaped section.
4. The aerodynamic studies of structures with a slight difference from the cross-section shapes, given in the standard and reference works, should be conducted.

References

1. Gosteev, Y., Konovalov, I., Lebedev, A., Obukhovskiy, A., Salenko, S., Yashinov, A. Numerical and Experimental Studies of the Use of Fiber-Reinforced Polymers in Long-Span Suspension Bridges. Energies. 2022. 15(5). Article no. 1864. DOI: 10.3390/en15051864
2. Gosteev, Yu.A., Obuhovskiy, A.D., Salenko, S.D. Influence of the shape on aerodynamic characteristics of girder bridges. Magazine of Civil Engineering. 2014. 5. Pp. 63–72. DOI: 10.5862/MCE.49.7
3. Kazakevich, M.I. Aerodinamicheskaia ustoichivost' nadzemnykh i visiachikh truboprovodov [Aerodynamic stability of above-ground and suspended pipelines]. Moscow: Nedra, 1977. 200 p.
4. Devnin, S.I. Aerogidromekhanika plokhoobtekaemykh konstruktsii [Aerohydromechanics of poorly streamlined structures]. Leningrad: Sudostroenie, 1983. 331 p.
5. Novak, M. Galloping Oscillations of Prismatic Structures. Journal of Engineering Mechanics Division. 1972. 98(1). Pp. 27–46. DOI: 10.1061/JMCEA3.0001575
6. Mannini, C., Marra, A.M., Bartoli, G. VIV–galloping instability of rectangular cylinders: Review and new experiments. Journal of Wind Engineering and Industrial Aerodynamics. 2014. 132. Pp. 109–124. DOI: 10.1016/j.jweia.2014.06.021
7. Larsen, A., Larose, G.L. Dynamic wind effects on suspension and cable-stayed bridges. Journal of Sound and Vibration. 2015. 334. Pp. 2–28. DOI: 10.1016/j.jsv.2014.06.009
8. Chen, W.-L., Zhang, Q.-Q., Li, H., Hu, H. An experimental investigation on vortex induced vibration of a flexible inclined cable under a shear flow. Journal of Fluids and Structures. 2015. 54. Pp. 297–311. DOI: 10.1016/j.jfluidstructs.2014.11.007
9. Li, M., Li, S., Liao, H., Zeng, J., Wang, Q. Spanwise correlation of aerodynamic forces on oscillating rectangular cylinder. Journal of Wind Engineering and Industrial Aerodynamics. 2016. 154. Pp. 47–57. DOI: 10.1016/j.jweia.2016.04.003
10. Daniotti, N., Jakobsen, J.B., Snæbjörnsson, J., Cheynet, E., Wang, J. Observations of bridge stay cable vibrations in dry and wet conditions: A case study. Journal of Sound and Vibration. 2021. 503. Article no. 116106. DOI: 10.1016/j.jsv.2021.116106
11. Yangchen, D., Shouying, L., Zhengqing, C. Experimental investigation on wake-induced vibrations of the hangers of suspension bridges based on three-dimensional elastic test model. Engineering Structures. 2021. 234. Article no. 111985. DOI: 10.1016/j.engstruct.2021.111985
12. Wang, B., Zhang, M., Xu, F. Experimental investigation on the vortex-induced vibration of a rectangular 4:1 cylinder under skew winds. Journal of Wind Engineering and Industrial Aerodynamics. 2022. 229. Article no. 105114. DOI: 10.1016/j.jweia.2022.105114
13. Ge, Y., Zhao, L., Cao, J. Case study of vortex-induced vibration and mitigation mechanism for a long-span suspension bridge. Journal of Wind Engineering and Industrial Aerodynamics. 2022. 220. Article no. 104866. DOI: 10.1016/j.jweia.2021.104866
14. Haque, M.N., Katsuchi, H., Yamada, H., Nishio, M. Investigation of Flow Fields Around Rectangular Cylinder Under Turbulent Flow by LES. Engineering Application of Computational Fluid Mechanics. 2014. 8(3). Pp. 396–406. DOI: 10.1080/19942060.2014.11015524
15. Fujino, Y., Kimura, K., Tanaka, H. Wind Resistant Design of Bridges in Japan: Developments and Practices. Springer. Tokyo, 2012. 256 p. DOI: 10.1007/978-4-431-54046-5
16. Elshaer, A., Bitsuamlak, G., Damatty, A. Aerodinamic optimization to reduce wind loads on tall building. Resilient Infrastructure. 2016. June. Article no. NDM-530.
17. Gao, D.-L., Chen, W.-L., Li, H., Hu, H. Flow around a slotted circular cylinder at various angles of attack. Experiments in Fluids. 2017. 58. Article no. 132. DOI: 10.1007/s00348-017-2417-8
18. Chen, W.-L., Gao, D.-L., Yuan, W.-Y., Li, H., Hu, H. Passive jet control of flow around a circular cylinder. Experiments in Fluids. 2015. 56. Article no. 201. DOI: 10.1007/s00348-015-2077-5
19. Carassale, L., Freda, A., Marrè-Brunenghi, M. Experimental investigation on the aerodynamic behaviour of square cylinders with rounded corners. Journal of Fluids and Structures. 2014. 44. Pp. 195–204. DOI: 10.1016/j.jfluidstructs.2013.10.010
20. Wang, Q., Jiang, Q., Hu, G., Chen, X., Li, C., Xiao, Y. Aerodynamic characteristics of a square cylinder with corner fins. Advanced in Bridge Engineering. 2021. 2. Article no. 20. DOI: 10.1186/s43251-021-00042-x
21. Ding, F., Kareem, A. Tall Buildings with Dynamic Facade Under Winds. Engineering. 2022. 6(12). Pp. 1443–1453. DOI: 10.1016/j.eng.2020.07.020
22. Shmigirilov, R., Ryabinin, A. Vliyaniye kontsevykh shayb na poperechnoye obtekaniye pryamougolnoy plastiny malogo udlineniya [Influence of end plates on the transversal flow past rectangular plate of small aspect ratio]. Estestvennye i matematicheskie nauki v sovremennom mire [Natural and mathematical sciences in the modern world]. 2015. 5(29). Pp. 158–162.
23. Zhou, S., Zou, Y., Hua, X., Liu, Z. Comparison of Two-Dimensional and Three- Dimensional Responses for Vortex-Induced Vibrations of a Rectangular Prism. Applied Sciences. 2020. 10(22). Article no. 7996. DOI: 10.3390/app10227996
24. Lyusin, V.D., Ryabinin, A.N. Issledovanie vliianiia udlineniia prizmy na ee aerodinamicheskie kharakteristiki i amplitudu kolebanii pri galopirovanii [Investigation of the influence of an elongated prism on its aerodynamic characteristics and vibration amplitude during galloping]. Vestnik of Saint Petersburg University. Mathematics. Mechanics. Astronomy. 2011. 2. Pp. 139–145.

Information about the authors:

Yuri Gosteev, *PhD in Physics and Mathematics*
E-mail: gosteev@corp.nstu.ru

Ilya Konovalov,
E-mail: iluhster@mail.ru

Alexander Obuhovskiy, *PhD in Technical Sciences*
E-mail: agd@craft.nstu.ru

Sergey Salenko, *Doctor of Technical Sciences*
E-mail: salenkosd@yandex.ru

Received: 25.09.2023. Approved: 05.05.2025. Accepted: 06.05.2025.